# The Al-Be (Aluminum-Beryllium) System

26.98154 9.01218

By J. L. Murray and D. J. Kahan
National Bureau of Standards

## Equilibrium Diagram

The phase diagram (Fig. 1) does not differ greatly from previous evaluations [Hansen, Mondolfo, 80Ell]. The detailed shape of the liquidus has been improved by taking thermodynamic data into account. The three-phase equilibria and pure metal transformations defining the topology of the phase diagram are summarized in Table 1.

The equilibrium solid phases of the Al-Be system are (1) the fcc (Al) solid solution containing up to 0.3 ± 0.1 at.% Be; (2) the low-temperature cph (αBe) solid solution, stable up to approximately 1254 °C and containing less than ~0.007 at.% Al; and (3) the high-temperature bcc (βBe) solid solution, stable between 1254 °C and its melting point.

**The Al-Rich Liquidus and the Eutectic Equilibrium.** The eutectic reaction occurs at a liquid composition of 2.5 ± 0.2 at.% Be and 644 ± 1 °C. The (Al) branch of the liquidus is approximately a straight line between the melting point of Al and the eutectic point. Experimental determinations of the Al-rich liquidus and eutectic temperature are summarized in Table 2. The assessed (Al) liquidus and eutectic point agree with the thermal analysis and microscopic work of [28Arc]. This work is compatible with the melting point of pure Al, with those thermodynamic properties of Al that determine the slope of the liquidus, and also with the (Be) liquidus, which must intersect the (Al) liquidus at the eutectic point. The Al-rich liquidus as drawn in Fig. 1 is taken from a thermodynamic calculation, described below, which is consistent

**Table 1 Three-Phase Equilibria and Pure Component Transformations**

| Phases | Compositions, at.% Be | | | Temperature, °C | Type |
|---|---|---|---|---|---|
| L ⇄ (Al) + (αBe) | 2.5 ± 0.2 | 0.3 ± 0.1 | >99.993 | 644 ± 1 | Eutectic |
| L − (αBe) − (βBe) | ~98 | ··· | >99.993 | ~1254 | Unknown |
| **Pure component transformations** | | | | | |
| L ⇄ (Al) | | 0 | | 660.5 | ··· |
| L ⇄ (βBe) | | 100 | | 1289 | ··· |
| (βBe) ⇄ (αBe) | | 100 | | 1254 | ··· |

**Fig. 1 Al-Be Phase Diagram**

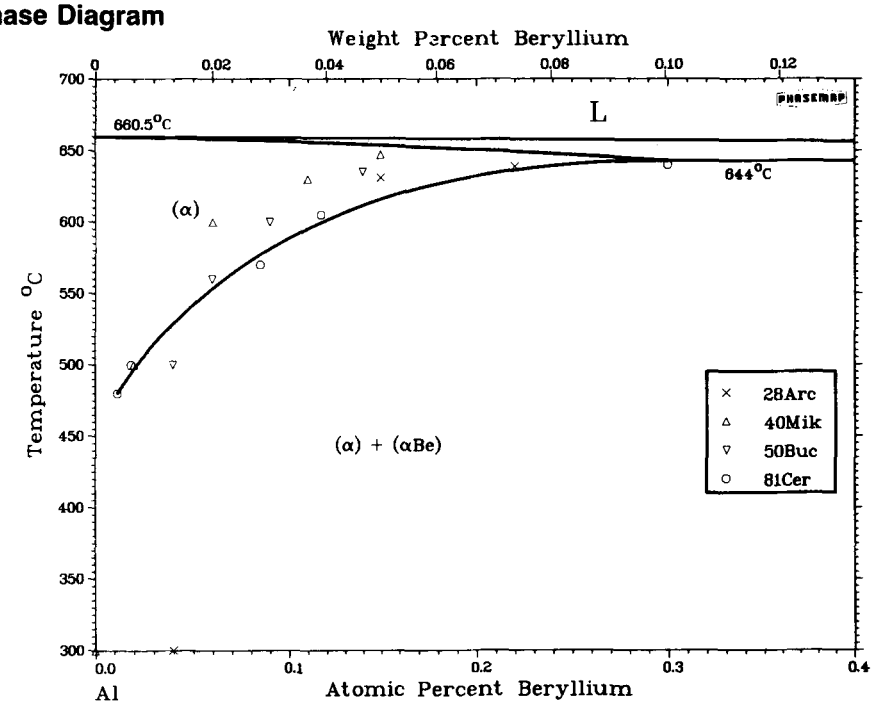


The assessed Al-Be diagram, together with experimental data on the liquidus. The numerical values shown are the assessed values. The drawn curves are from the thermodynamic calculations and their positions do not always correspond exactly to the assessed values; see text.
J. L. Murray and D. J. Kahan, 1983.

**Table 2 The Al-Rich Liquidus**

| Reference | Liquidus Composition, at.% Be | Liquidus Temperature, °C | Method |
|---|---|---|---|
| [16Oes] | 0 | 658 | Thermal analysis, heating and cooling |
| | 1.18 | 654 | |
| | 2.34 | 650 | |
| | ~4.1 | 644(a) | |
| [26Kro] | 4.1 | 640(a) | Metallography |
| [28Arc] | 2.55 | 645(a) | Metallography, thermal analysis |
| [30Haa] | 4.1 | 647(a) | Metallography |
| [40Los] | 0.15 | 655.8 | Thermal analysis (cooling) |
| | 0.26 | 654.7 | |
| | 0.37 | 652.2 | |
| | 0.70 | 651 | |
| | 1.47 | 648.1 | |
| | 2.17 | 646 | |
| | 3.4 | 644.5 ±0.3(a) | |
| [40Mik] | 0.3 | 660.3 | Thermal analysis |
| | 0.6 | 657.1 | |
| | 0.75 | 656.5 | |
| | 0.95 | 654.0 | |
| | 1.19 | 651.0 | |
| | 1.5(a) | 647.0 | |

(a) Eutectic.

with the chosen experimental data. The calculated eutectic composition and temperature are 2.34 at.% Be and 643 °C.

For Al-rich compositions, a congruent melting of (Al) and peritectic reaction L + ($\alpha$Be) → (Al) was suggested by [66Nis], at variance with the eutectic reaction found by all other investigators. The peritectic reaction is not accepted, because eutectic microstructures have been established by other work (e.g., [63Hin, 28Arc]) and also because it is inconsistent with the accepted (Al) solvus data.

**Be-Rich Liquidus.** The melting point of $\beta$Be is 1289 °C [81BAP]. Liquidus determinations were made by [16Oes, 40Los, 40Mik, 66Nis, 67Pot]; the experimental data are summarized in Table 3. In the range 2.5 to 40 at.% Be, various determinations (except [40Mik]) agree within 2 to 3 at.% at a given temperature. The assessed liquidus is the result of thermodynamic optimizations using data of [16Oes, 40Los, 66Nis, 67Pot]; details of the calculation are described below.

For Be contents greater than 40 at.%, thermal analysis results of [16Oes] and [40Los] disagree by 30 to 60 °C. On the one hand, there is some evidence that [40Los] should be preferred: [16Oes] used materials of unknown purity, and they also reported undercoolings of 10 to 20 °C in the Be-rich alloys. [40Los] claimed to have maintained very high purity of his alloys and examined the effect of cooling rate on thermal analysis results. On the other hand, the evidence against choosing the higher melting points is: [40Los] reported that the maximum solubility of Al in ($\beta$Be) was approximately 1.7 at.%, far greater than the accepted value. Also, the higher melting points appear to conflict with the thermodynamic data on this system.

[Hansen] based the Be-rich part of the liquidus on averages of the two sets of data. We have examined the consistency of the liquidus data with thermodynamic data for this system. Using the estimated enthalpies and entropies due to [Hultgren, Elements], we calculated liquidus curves

**Table 3 Experimental Data for the Be-Rich Liquidus**

| Reference | Liquidus Composition, at.% Be | Liquidus Temperature, °C | Method |
|---|---|---|---|
| [16Oes] | 2.4 | 650 | Thermal analysis (cooling and heating) |
| | 6.3 | 758 | |
| | 11.0 | 855 | |
| | 20.6 | 996 | |
| | 36.2 | 1083 | |
| | 56.0 | 1130 | |
| | 71.3 | 1148 | |
| | 87.7 | 1175 | |
| | 95.0 | 1214 | |
| | 97.0 | 1230 | |
| [40Los] | 2.2 | 646 | Thermal analysis (cooling) |
| | 6.1 | 738 | |
| | 8.5 | 802 | |
| | 15.7 | 912 | |
| | 31.9 | 1026 | |
| | 55.5 | 1158 | |
| | 76.2 | 1205 | |
| | 81.0 | 1216 | |
| | 90.4 | 1248 | |
| | 96.4 | 1270 | |
| [66Nis] | 3.1 | 671 | Metallography, thermal analysis |
| | 4.2 | 739 | |
| | 6.0 | 777 | |
| | 8.0 | 798 | |
| | 90.4 | 1248 | |
| [67Pot] | 3.1 | 650 | Chemical analysis of liquid in equilibrium with (Be) |
| | 4.0 | 690 | |
| | 5.6 | 735 | |
| | 9.8 | 810 | |
| | 11.9 | 840 | |
| | 15.0 | 880 | |
| | 21.3 | 940 | |
| | 26.6 | 1000 | |
| | 33.0 | 1055 | |
| | 38.7 | 1100 | |
| [40Mik] | 2.4 | 659 | Thermal analysis (cooling) |
| | 4.0 | 670 | |
| | 6.9 | 675 | |
| | 11.4 | 694 | |

that agree with the data of [16Oes] and are not consistent with those of [40Los]. We have slightly adjusted our estimates of the enthalpy and entropy of melting so that the data of [16Oes] lie below the calculated liquidus curve at compositions greater than 75 at.% Be. The liquidus of Fig. 1 is the result of the optimizations described in the section entitled "Thermodynamics". Above 1100 °C, the liquidus merits further experimental investigation.

**Solubility of Be in (Al).** The maximum solubility of Be in (Al) is 0.3 ± 0.1 at.% Be at the eutectic temperature [81Cer]. Experimental data on the solubility of Be in (Al) are shown in Table 4 and Fig. 2.

Metallographic determination of the solvus is hampered by the very low solubility and the difficulty in polishing soft samples [28Arc]. The solubilities reported by [30Haa, 37Mak, 40Los, 66Nis], as previously pointed out by [Hansen], are certainly too high. The most accurate methods (lattice parameters, resistivity, and microhardness) [28Arc], [40Mik], [46Buc], [50Buc], and [81Cer] gave lower solubilities, and these studies agreed well with one another. The data of [81Cer] are preferred because of their consistency with an Arrhenius relationship, which is expected for systems of small solubility.

**Fig. 2 Solubility of Be in (Al)**

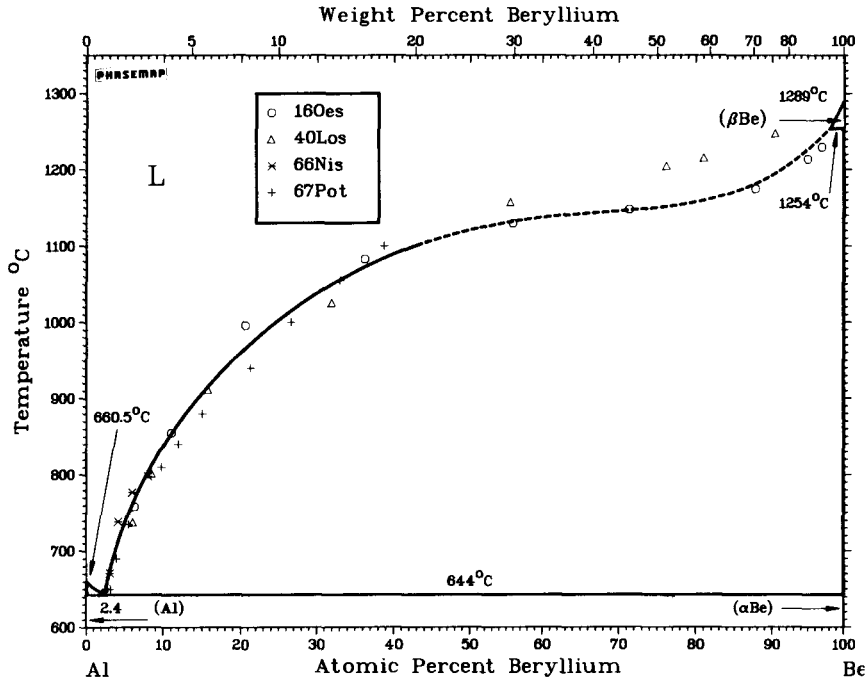


**Note:** The numerical values shown are the assessed values. The drawn curves are from thermodynamic calculations and their positions do not always correspond exactly to the assessed values; see text. J. L. Murray and D. J. Kahan, 1983.

**Table 4 (Al) Solvus Data**

| Reference | Temperature, °C | Composition, at.% Be | Experimental method |
|---|---|---|---|
| [81Cer] | 640 | 0.30 | Resistivity |
| | 605 | 0.117 | |
| | 570 | 0.085 | |
| | 500 | 0.0186 | |
| | 480 | 0.0115 | |
| [28Arc] | 639 | 0.22 | Hardness |
| | 631 | 0.15 | |
| | ~300 | <0.04 | |
| [40Mik] | 647 | 0.15 | Lattice parameters |
| | 630 | 0.11 | |
| | 600 | 0.06 | |
| | 500 | 0.02 | |
| | ~300 | ~0 | |
| [46Buc] | 645 | 0.19 | Microhardness |
| | 635 | 0.14 | |
| | 600 | 0.07 | |
| | 500 | 0.03 | |
| | 400 | 0.02 | |
| [50Buc] | 635 | 0.14 | Microhardness, diffusion |
| | 600 | 0.09 | |
| | 560 | 0.06 | |
| | 500 | 0.04 | |
| [71Ser] | 645 | 0.19 | emf (calculated) |
| [30Haa] | 647 | 2.4 | Metallography, dilatometry |
| [37Mak] | 610 | 0.42 | Lattice parameters |
| [40Los] | 644 | ~0.9 | Resistivity |
| | ~300 | ~0.3 to 0.4 | |
| [66Nis] | ~646 | ~3 | Metallography |

**Solubility of Al in (αBe) and (βBe).** The maximum solubility of Al in (αBe) is less than 0.007 at.% [76Mye]. Earlier work also is consistent with this upper bound (see Table 5). The only differing report is [40Los], which has been discounted because of the irreproducibility of their resistivity measurements [50Kau], as well as because of the purer Be and more sensitive analysis used in the recent measurements.

**Table 5 Data on the Maximum Solubility of Al in (Be)**

| Reference | Composition at.% Al | Composition at.% Be | Method |
|---|---|---|---|
| [76Mye] | <0.007 | >99.993 | Ion-beam implantation |
| [68Jac] | <0.02 | >99.98 | Electron microprobe |
| [65Ham] | ~0.02 | ~99.98 | Electron microprobe (630 °C) |
| [63Hin] | <0.03 | >99.97 | X-ray |
| [50Kau] | <0.3 | >99.7 | Metallography |
| [37Mak] | <0.3 | >99.7 | Lattice parameters |
| [26Kro] | <0.6 | >99.4 | Metallography |
| [40Los] | ~1.7 | ~98.5 | Resistivity |

[65Ham] and [68Jac] noted that their value of ~0.02 at.% Al (at 15 °C below the eutectic temperature) was at the limit of detectability, with errors of the same order as the measured concentrations. Similarly, [76Mye] found the solubility to be below the limit of detectability, and the upper bound of 0.007 at.% Al is based on impurities of the starting materials and experimental uncertainties. [76Mye] verified the precipitation of (Al) by TEM measurements.

In view of the exceedingly low solubility of Al in (αBe) up to 800 °C, the effect of Al on the (αBe) ⇄ (βBe) transformation can probably be assumed to be negligible.

## Metastable Phases

**Guinier-Preston Zones.** Al-rich alloys are age-hardening [28Arc, 68Cer]. [68Cer] found evidence that the decomposition of supersaturated (Al) solid solutions involves the formation of Guiner-Preston (G. P.) zones, or solute clustering, by means of a resistometric study of quenching and isochronal and isothermal aging of a 0.03 at.% Be alloy. [81Cer] made further resistivity measurements in order to redetermine the equilibrium solvus and to estimate the position of the coherent G. P. solvus. [81Cer] then used small-angle X-ray scattering (SAXS) to estimate the composition of solute clusters as a function of aging temperature. After aging at 20, 60, 100, and 140 °C, the matrix compositions were estimated to be 0.0115, 0.0139, 0.0163, and 0.0186 at.% Be, and the compositions of the G. P. zones were estimated to be 48, 40.5, 31, and 23 at.% Be, respectively. Although the formation of G. P. zones has been demonstrated, the compositions of the precipitates must be considered to be approximate. From the SAXS data, [81Cer] deduced that the precipitates have the form of platelets.

**Rapid Quenching.** [76Pet] proposed that vapor-deposited Al-Be alloy films with Be content greater than 3 at.% are amorphous. This result was based on the composition dependence of the superconducting transition temperature, $T_c$: the steep decrease of $T_c$ with decreasing Be content near pure Al was taken as evidence of a change from the amorphous to the crystalline state.

The structure of vapor-deposited Be-rich alloys, however, is controversial, because of disagreement concerning the structure of vapor-deposited pure Be [61Laz, 66Fuj, 76Pet, 82Glo]. Several noncrystalline low-temperature phases in Be were reported [61Laz, 66Fuj], but when the purity of the Be is carefully maintained, cph crystals are observed [82Glo]. [76Pet] interpreted $T_c$ data as indicating that no crystalline-to-amorphous transition occurs with increasing Al content.

Ultra-rapid liquid quenching was carried out on alloys containing 2.9, 13.6, and 92.3 at.% Be [62Jor]. After rapid quenching, no new phases were found; only Al was detected in the first two samples, and only Be and Al in the third. [62Jor] did not propose that any extensions of the solid solubilities were obtained, because they did not consider significant the slight differences in the lattice parameters before and after quenching.

## Crystal Structures and Lattice Parameters

Crystal structures and lattice parameters are summarized in Tables 6 and 7. Data on the lattice parameters, structures, and transformation temperature of pure Be are from [Pearson].

## Thermodynamics

**Experimental Thermodynamic Work.** [67Bie], [69Sch], and [71Ser] determined thermodynamic properties of Al-Be alloys. [71Ser] measured the activity of Be in liquid Al-rich alloys by the emf method. The liquid was found to obey Henry's law. The excess partial enthalpy, entropy, and Gibbs energy of the Be-rich liquid at infinite dilution were reported as 26.4 ± 2.9 kJ/mol, 2.9 ± 2.9 J/mol·K, and 23.8 ± 0.8 kJ/mol, respectively, at 1000 K.

[69Sch] measured the activities of both Al and Be in the liquid between 1653 and 1760 K, using the Knudsen effusion method. Values for $\Delta H_{Be}$ and $\Delta S_{Be}$ were derived using phase diagram data and a van Laar model for the liquid Gibbs energy. These data are tabulated in [Hultgren]. Integral excess enthalpies and entropies were given by [69Sch], but Hultgren pointed out that these quantities were not experimentally verified and should be considered to be only approximate. Data of [69Sch] were used as input to the optimization calculations to be described below.

[67Bie] reported the limiting value of the activity coefficient for Al in liquid Be as 4.64 at 1600 K, based on emf measurements. The present calculations are consistent with this result: for ln $\gamma_{Be}$, we calculated 20.42 kJ/mol, compared to 20.40 kJ/mol [67Bie].

**Thermodynamic Calculations.** Optimizations of the liquid Gibbs energy were performed using liquidus data, both alone and together with partial Gibbs energy and excess entropy data [69Sch]. The input data are divided into four subsets:

- Liquidus data below 1100 °C, for which most investigations are in agreement and which are easily reproduced by thermodynamic calculations
- The liquidus above 1100 °C, for which there are few data, with large discrepancies
- Partial Gibbs energies of both components at 1600 K, for which [Hultgren] assigned error estimates of ±420 J/mol
- Integral excess entropies, which are considered to be very uncertain

**Table 6 Al-Be Crystal Structure Data**

| Phase | Equilibrium composition range, at.% Be | Pearson symbol | Strukturbericht designation | Space group | Prototype |
|---|---|---|---|---|---|
| (Al) | 0-0.30 | *cF4* | *A1* | *Fm3m* | Cu |
| (βBe)(a) | 99.993-100 | *cI2* | *A2* | *Im3m* | W |
| (αBe)(b) | 99.993-100 | *hP2* | *A3* | $P6_3/mmc$ | Mg |

(a) High-temperature form. (b) Low-temperature form.

**Table 7 Lattice Parameters of Equilibrium Phases**

| Phase | Lattice parameters, nm *a* | *c* | Composition, at.% Be | Temperature, °C | Reference |
|---|---|---|---|---|---|
| (Al) | 0.40496 | ··· | 0 | 25 | [Landoldt-Börnstein] |
| (βBe) | 0.25515 | ··· | 100 | 1254 | [61Amo] |
| (αBe) | 0.22866 | 0.35833 | 100 | 22 | [Landoldt-Börnstein] |

**Table 8 Thermodynamic Parameters, J/mol, J/mol · K**

$G_{Al}$ (fcc) = 10711 − 11.506 $T$
$G_{Be}$ (cph) = 17805 − 11.506 $T$
$G_{Be}$ (bcc) = 10457 − 6.694 $T$

| Fig. 1 (liquidus data) | Liquidus and thermochemical data |
|---|---|
| $B_L$ = 49870 − 22.92 $T$ | $B_L$ = 56151 − 29.12 $T$ |
| $C_L$ = −7202 | $C_L$ = −4491 − 3.27 $T$ |

Optimizations using all the data, including excess entropies, succeed in matching the liquidus below 1000 °C, but lead to errors in the liquidus above 1000 °C and to errors in $G_{Al}$ that are outside the assigned limits. Integral entropy data were, therefore, not used for further optimizations.

An optimization based on the partial Gibbs energies of [69Sch] leads to a Gibbs energy not very different from an optimization based on liquidus data alone. The results of the two calculations are compared in Table 8. The liquidus resulting from the calculation based only on liquidus data was used to draw the diagram, because above 1100 °C it more nearly approximates the available liquidus data. The calculated eutectic temperature and composition are 643 °C and 2.34 at.% Be, and the temperature and composition of the critical point of the metastable liquid miscibility gap are 1100 °C and 68 at.% Be. For the purpose of extrapolating to ternary systems or calculating thermodynamic quantities, however, the results of calculations based on the partial Gibbs energies of [69Sch] are preferred.

**Model Gibbs Energy Functions.** The Gibbs energy of the liquid phase is represented as:

$$G^i = RT(x \ln x + (1 - x) \ln(1 - x)) + B^i x(1 - x) + C^i x(1 - x)(1 - 2x)$$

where $i$ designates the phase; $x$, the atomic fraction of Be; and $B^i$ and $C^i$, the interaction parameters.

For the purpose of thermodynamic calculations, we have assumed that the mutual solubilities of Al and Be in the solid phases are zero and have calculated only the liquidus. The Gibbs energies of solid phases are described by lattice stability parameters. Lattice stability parameters were derived from enthalpies and entropies of melting given by [Hultgren, Elements].

None of the calculations reproduced Hansen's liquidus at compositions greater than 70 at.% Be, because this part of the liquidus is sensitive primarily to the entropy and enthalpy of melting of pure ($\alpha$Be), which were fixed. Because these quantities were not determined experimentally, but estimated by [Hultgren, Elements], these quantities were also varied in an optimization. The resulting values reproduced Hansen's liquidus except that the melting point of metastable ($\alpha$Be) was higher than that of the stable phase. This is not allowed by thermodynamic considerations. We concluded that thermodynamic calculations can be used as a criterion for preferring the liquidus data of [16Oes] to that of [40Los].

## Cited References


***16Oes:** G. Oesterheld, "Melting Point and Heat of Fusion of Beryllium; Alloys of Beryllium with Aluminum, Copper, Silver and Iron", *Z. Anorg. Chem., 97,* 9-14 (1916) in German. (Equi Diagram)

**26Kro:** W. Kroll, "Substitution of Silicon by Beryllium", *Metall und Erz., 22,* 613-616 (1926) in German. (Equi Diagram)

***28Arc:** R.S. Archer and W.L. Fink, "Aluminum-Beryllium Alloys", *Trans. AIME, 78,* 616-643 (1928). (Equi Diagram)

**30Haa:** M. Haas and D. Uno, "Contribution to the Hardening Phenomenon in Beryllium-Aluminum and Magnesium-Aluminum Alloys", *Z. Metallkd., 22,* 277-279 (1930) in German. (Equi Diagram)

**37Mak:** E.S. Makarov and L. Tarschisch, "X-Ray Studies of the Al-Be Phase Diagram", *Zh. Fiz. Khim., 9*(3), 350-358 (1937) in Russian. (Crys Structures, Equi Diagram)

**40Los:** L. Losana, "The Beryllium-Aluminum System", *Alluminio, 9,* 8-13 (1940) in Italian. (Equi Diagram, Meta Phases)

**40Mik:** V.I. Mikheeva, "The Solubility of Beryllium in Aluminum", *Izv. Akad. Nauk SSSR Otd. Khim. Nauk, 5,* 775-782 (1940) in Russian. (Equi Diagram, Crys Structures)

**46Buc:** H. Buckle, "Solubility Determination by Micro-Hardness Examination", *Z. Metallkd., 37,* 43-47 (1946) in German. (Equi Diagram)

**50Buc:** H. Buckle and J. Descamps, "Micro-Hardness Study of Diffusion of Beryllium in Very Pure Aluminum", *C.R. Acad. Sci., 230,* 752-754 (1950) in French. (Equi Diagram)

**50Kau:** A.R. Kaufman, P. Gordon, and D.W. Lillie, "The Metallurgy of Beryllium", *Trans. ASM, 42,* 785-844 (1950). (Equi Diagram)

**61Amo:** V.M. Amonenko, V.Ye. Ivanov, G.F. Tikhinskii, V.A. Finkels, and I.V. Shpagin, "High-Temperature Polymorphism of Beryllium", *Fiz. Met. Metalloved., 12*(6), 865-871 (1961) in Russian; TR: *Phys. Met. Metal., 12*(6), 77-83 (1961). (Equi Diagram)

**61Laz:** B.G. Lazarev, E.E. Semenenko, and A.I. Sudovtsov, "Modifications of Beryllium and Iron in Films Condensed onto Cold Substrates", *J. Exptl. Theoret. Phys., 40,* 105-108 (1961) in Russian; TR: *Sov. Phys. JETP, 13,* 75-77 (1961). (Meta Phases)

**62Jor:** C. Jordan, "Investigation of the Effect of Ultra-Rapid Quenching on Metallic Systems, Including Beryllium Alloys", Tech. Rept. ASD-TDR-62-181, Wright Patterson AFB, 16 (1962).

**63Hin:** E.D. Hindle and G.F. Slattery, "The Metallurgy of Beryllium", *Inst. of Metals Monograph Rept. Ser.,* (28), 651-664 (1963). (Equi Diagram)

**65Ham:** M.L. Hammond, A.T. Davinroy, and M.I. Jacobson, "Beryllium-Rich End of Five Binary Systems", Tech. Rept. AFML-TR-65-223, AD No. 468484, 30-33 (1965). (Equi Diagram)

**66Fuj:** S. Fujime, "Electron Diffraction at Low Temperature III. Radial Distribution Analysis of Metastable Structure of Metal Films Prepared by Low Temperature Condensation", *Jpn. J. Appl. Phys., 5*(9), 778-787 (1966). (Meta Phases)

**66Nis:** S. Nishi, "Study on Binary Diagram of Al-Be Alloy", *Light Metals Jpn., 16,* 5-8 (1966) in Japanese. (Equi Diagram)

**67Bie:** G. Bienvenu, C. Potard, B. Schaub, and P. Desre, "Determination of the Thermodynamic Activity of Iron, Nickel, Aluminum and Copper in Dilute Solutions in Liquid Beryllium", *Thermodynamics of Nuclear Materials,* Proc. IAEA Conf., Vienna, 777-787 (1967) in French. (Thermo)

**67Pot:** C. Potard, G. Bienvenu, and B. Schaub, "A Study of the Distribution of Iron, Copper and Molybdenum Impurities Between the Solid and Liquid Phases in Aluminum-Beryllium Alloys", *Thermodynamics of Nuclear Materials,* Proc. IAEA Conf., Vienna, 809-825 (1967) in French. (Thermo, Equi Diagram)

**68Cer:** S. Ceresara, T. Federighi, and P. Fiorini, "Clustering in Al-Be 0.1% Alloy", *Philos. Mag., 18,* 49-54 (1968). (Crys Structure)

**68Jac:** M.I. Jacobson and M.L. Hammond, "The Solid Solubilities of Silver, Aluminum, Chromium, Copper, and Iron in Zone-Refined Beryllium", *Trans. Met. Soc. AIME, 242,* 1385-1391 (1968). (Equi Diagram)

***69Sch:** B. Schaub, C. Potard, and P. Desre, "Thermodynamic Study of the Be-Al System", Proc. 1st Intl. Conf. Calorimetry and Thermodynamics, Warsaw, 1011-1013 (1969). (Thermo)

**71Ser:** G.A. Serebryakov, V.A. Lebedev, I.F. Nichkov, S.P. Raspopin, and E.A. Novikov, "Thermodynamics of the Interaction Between Beryllium and Aluminum", *Zh. Fiz. Khim.,* (8),

2092-2094 (1971) in Russian; TR: *Russ. J. Phys. Chem.*, 45(8), 1186-1187 (1971). (Thermo, Equi Diagram)

**76Mye:** S. M. Myers and J. E. Smugeresky, "Phase Equilibria and Diffusion in the Be-Al-Fe System Using High-Energy Ion Beams", *Met. Trans., 7A*, 795-802 (1976). (Equi Diagram)

**76Pet:** J. Petersen, "Superconducting Transition Temperatures of Amorphous Binary Alloy Systems Based on Bi, Pb, Ga and Be", *Z. Phys., B24*, 273-278 (1976). (Meta Phases)

**80Ell:** R. P. Elliott and F. A. Shunk, "Evaluation of the Al-Be (Aluminum-Beryllium) System", *Bull. Alloy Phase Diagrams, 1*(1), 49-50 (1980). (Equi Diagram; Review)

**81BAP:** "Melting Points of the Elements (IPTS-68)", *Bull. Alloy Phase Diagrams, 2*(1), 145-146 (1981).

***81Cer:** S. Ceresara, "Determination of the Miscibility Gap in the Al-Be System by Resistivity Measurements and X-Ray Small-Angle Scattering", *Philos. Mag., 43A*, 1093-1101 (1981). (Equi Diagram, Meta Phases)

**82Glo:** R. E. Glover, III, private communication (1982). (Meta Phases)

*Indicates key paper.

Al-Be evaluation contributed by **J. L. Murray** and **D. J. Kahan,** Center for Materials Science, National Bureau of Standards. This work was jointly funded by the Defense Advanced Research Project Agency (DARPA) and the National Bureau of Standards through the Metallurgy Division and through the Office of Standard Reference Data. Literature searched through 1981. Dr. J. L. Murray and Dr. A. J. McAlister are the ASM/NBS Data Program Category Editors for binary aluminum alloys.

# The Al-Zn (Aluminum-Zinc) System

26.98154 65.38

**By J. L. Murray**
**National Bureau of Standards**

## Equilibrium Diagram

The single-phase fcc (Al) solid solution has an extended composition range, interrupted by a miscibility gap. The (Al) solid solution will sometimes be denoted $\alpha$ or $\alpha'$ to distinguish between Al- and Zn-rich compositions, respectively. The (Al) liquidus and solidus descend to a eutectic equilibrium with cph (Zn) at 381 °C, and at 277 °C a eutectoid (monotectoid) equilibrium of $\alpha$, $\alpha'$, and (Zn) occurs. Near equiatomic compositions, the (Al) solidus curve has an inflection caused by the nearness of the fcc miscibility gap. The three-phase equilibria and pure metal transformations that define the topology of the diagram are summarized in Table 1.

The liquidus, solidus, and solvus curves are well established. The most recent evaluation of the phase diagram [Elliott] represents ($\alpha'$Al) as separated into two distinct fcc phases, separated by a narrow two-phase region at 50 at.%. This two-phase region intersects the solidus at 443 °C and the ($\alpha$Al) miscibility gap at 340 °C. The present assessed diagram does not include these reactions and differs only slightly from the earlier version of [Hansen]. The metastable miscibility gap for the separation of coherent precipitates from supersaturated (Al) is established.

Early investigators (1897 to 1911) believed that there existed an intermetallic compound $AlZn_2$, based on thermal analysis work (proposed peritectic arrests at 443 °C). Later studies identified the second phase as an fcc solid solution. With time (1922 to 1935), the two-phase ($\alpha$ + $\alpha'$) region shrank to a very narrow range near 50 at.%. In 1938, the high-temperature part of the two-phase region disappeared, leaving a monotectoid reaction. By means of high-temperature lattice parameter and resistivity measurements, a smooth miscibility gap was defined, with a critical temperature of 351 °C [Hansen].

In 1961 and 1963, the observation of anomalies in high-temperature lattice parameters led to the reinstatement of a very narrow two-phase region ($\alpha$ + $\alpha'$) at 50 at.%, and a diagram almost identical to that of [24Tan]. Accurate definition of the two-phase region was not pursued further. Such a recantation leaves one with several difficulties. The intersection of the two-phase region with the solidus was put back at 443 °C, and the evidence against such a three-phase equilibrium is strong. The two-phase region cannot be reconciled with previous determinations of the miscibility gap. Finally, the proposed two-phase region separates two structurally identical fcc solid solution phases of nearly equal compositions, and this is thermodynamically implausible.

**The Liquidus.** Aluminum melts at 660.45 °C and Zn at 419.6 °C [81BAP]. The phase diagram is of the eutectic type; the eutectic temperature and composition are 381 ± 1 °C and 88.7 ± 0.2 at.% Zn. Reported eutectic temperatures range from 380.5 °C [1897Hey] to 382 °C [39Mor]; reported eutectic compositions range from 88.5 to 89.5 at.% Zn. Tables 2, 3, and 4 summarize experimental determinations of the eutectic point and liquidus.

**Table 1 Special Points in the Al-Zn Phase Diagram**

| Phases | Compositions, at.% Zn | | Temperature, °C | Type |
|---|---|---|---|---|
| L ⇄ ($\alpha'$Al) + (Zn) | 88.7 | 67.0 | 381 | Eutectic |
| ($\alpha'$Al) ⇄ ($\alpha$Al) + (Zn) | 59 | 16.5 | 277 | Eutectoid |
| (Al) ⇄ ($\alpha$Al) + ($\alpha'$Al) | | 39.5 | 351.5 | Critical |
| L ⇄ (Al) | | 0 | 660.452 | Congruent |
| L ⇄ (Zn) | | 100 | 419.58 | Congruent |